 doi:10.20944/preprints201710.0141.v1

Article

A Case Study on Large deformation Failure Mechanism of Coal Given Chamber and invention of a new wall-mounted coal bunker in Xiashijie Coal Mine with Soft, Swelling Floor Rock

Xingkai Wang [1,2], Wenbing Xie [1,*], Shengguo Jing [2], Jianbiao Bai [1] and Zhili Su [2]

[1] State Key Laboratory of Coal Resources and Safe Mining, China University of Mining and Technology, Xuzhou 221116, China; xingkai10@163.com (X.W.); baijianbiao@cumt.edu.cn (J.B.)
[2] School of Mines, China University of Mining and Technology, Xuzhou 221116, China; 1039022122@qq.com (S.J.); suzhili@cumt.edu.cn (Z.S.)
* Correspondence: wb_xiewang@163.com; Tel.: +86-183-5134-3101

Abstract: Serious damage caused by floor heave in the coal given chamber of a vertical coal bunker is one of the challenges faced in underground coal mines. Engineering practice shows that it is more difficult to maintain the coal given chamber (CGC) than a roadway. More importantly, repairing the CGC during mining practice will pose major safety risks and reduce production. Based on the case of the serious collapse that occurred in the bearing structure of the CGC at the lower part of the 214# coal bunker in Xiashijie mine, China, this work analysed (i) the main factors influencing floor heave and (ii) the failure mechanism of the load-bearing structure in the CGC using FLAC^{2D} numerical models and expansion experiment. The analysis results indicate that: the floor heave, caused mainly by mine water, is the basic reason leading to the instability and repeated failure of the CGC in the 214# coal bunker. Then a new coal bunker, without building the CGC, is proposed and put into practice to replace the 214# coal bunker. The FLAC^{3D} software program is adopted to establish the numerical model of the wall-mounted coal bunker (WMCB), and the stability of the rock surrounding the WMCB is simulated and analysed. The results show that: (1) the rock surrounding the sandstone segment is basically stable. (2) The surrounding rock in the coal seam segment, which moves into the inside of the bunker, is the main zone of deformation for the entire rock mass surrounding the bunker. Then the surrounding rock is controlled effectively by means of high-strength bolt–cable combined supporting technology. According to the geological conditions of the WMCB, the self-bearing system, which includes (i) H-steel beams, (ii) H-steel brackets, and (iii) self-locking anchor cables, is established and serves as a substitute for the CGC to transfer the whole weight of the bunker to stable surrounding rock. The stability of the new coal bunker has been verified by field testing, and the coal mine has gained economic benefit to a value of 158.026174 million RMB over three years. The new WMCB thus made production more effective and can provide helpful references for construction of vertical bunkers under similar geological conditions.

Keywords: Vertical coal bunker; Coal given chamber; Floor heave; Wall-mounted coal bunker; Reinforcement; Self-bearing system

1. Introduction

The raw coal, produced at the working face of underground coal mine, should be transported to the surface by the transportation system which includes a coal strap transporting system in the mining roadway, a coal storage bunker installed in mining area, the conveyor belt in the main haulage roadway, a coal bunker at the bottom of shaft, and the main shaft hoisting system. It is clear that the storage bunker plays an indispensable role in coal transportation. In addition, the use

Preprints (www.preprints.org) | NOT PEER-REVIEWED | Posted: 20 October 2017 doi:10.20944/preprints201710.0141.v1

of bunkers can reduce the effect of transportation interruptions and congestion [1-2], increase mine system availability [3], and improve transportation efficiency [4-5]. The bunker usually contains a bottom coal bunker, district coal bunker, section coal bunker, ground bunker, and a tunnelling bunker [4]: these are generally divided into three forms: horizontal, vertical, or inclined. On the whole, horizontal coal bunkers are used widely in the United Kingdom, the USA, Canada, the former Soviet Union, *etc*. However, China, one of the earlier coal mining countries, has been committed to the research and construction of vertical coal bunkers [2].

The vertical bunker has been used widely in China for many years. Figure 1 (a) shows the structure of a traditional vertical bunker, it includes the coal bunker body, the coal given chamber which is constructed in the roadway and bears the whole weight of the coal inside the bunker, the concrete silo, and the coal feeder machine. The belt conveyors feed into the top of the bunker from either vibro-feeders or variable speed belt-feeders loading out at the bottom [6]. The stability of the coal given chamber is crucial to ensure the bunker works effectively. Here, the 214# coal bunker could not be used due to the severe floor heave in the coal given chamber (CGC), even though the CGC was repaired annually and effective measures had been taken to improve the stability of the load-bearing structure of the CGC. Figure 2 shows the large deformation caused by floor heave in the CGC where the floor strata is characterised by severe swelling.

The study of the existing literature focuses on: (i) the optimum bunker size and location selection in underground coal mine conveyor systems[3,7], (ii) the construction of the coal bunker with large diameter and high vertical height [8-9], (iii) the optimisation of methods of safe construction under different geological conditions [10-11], (iv) the deterioration and collapse mechanism of the reinforced concrete bunker [12], (v) the curing technique of blockage and fractures in the walls of the coal bunker body[13-15], and (vi) the maintenance of the coal bunker [16-18] and have made significant progress. However, there is no generally accepted theory applicable to construction of a new vertical coal bunker (Figure 1 (b)) without building coal given chamber, especially when the coal given chamber could not be built up on such loose, swelling floor rock. This work used field conveyor, theoretical analysis, laboratory tests, and numerical simulation to analyse the main factors influencing floor heave and the failure mechanism of the load-bearing structure in the CGC. Then a new coal bunker (a wall-mounted coal bunker), without building the CGC, was designed and its key technological bases were investigated. During the research into the new bunker, we focused on how to transfer the whole weight borne by the bearing structure of the CGC into the rock surrounding the coal bunker where we constructed the self-bearing system. Finally we discussed the security and the reliability of the new coal bunker and put it into practice at Xiashijie coal mine. Meanwhile we described the monitoring of the subsidence of the bunker body and the deformation of the bunker walls in a field test lasting for three years.

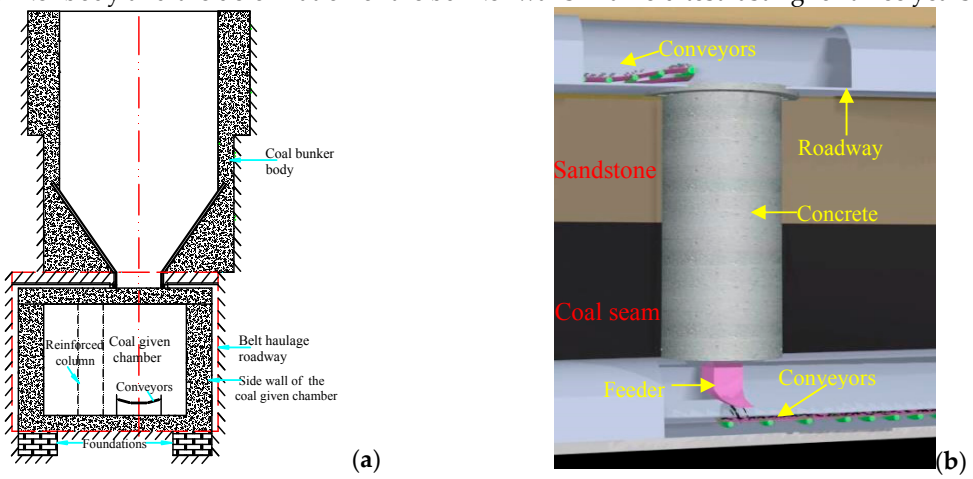

Figure 1. The structure of (**a**) the traditional vertical bunker and (**b**) the new vertical bunker.

Preprints (www.preprints.org) | NOT PEER-REVIEWED | Posted: 20 October 2017 doi:10.20944/preprints201710.0141.v1

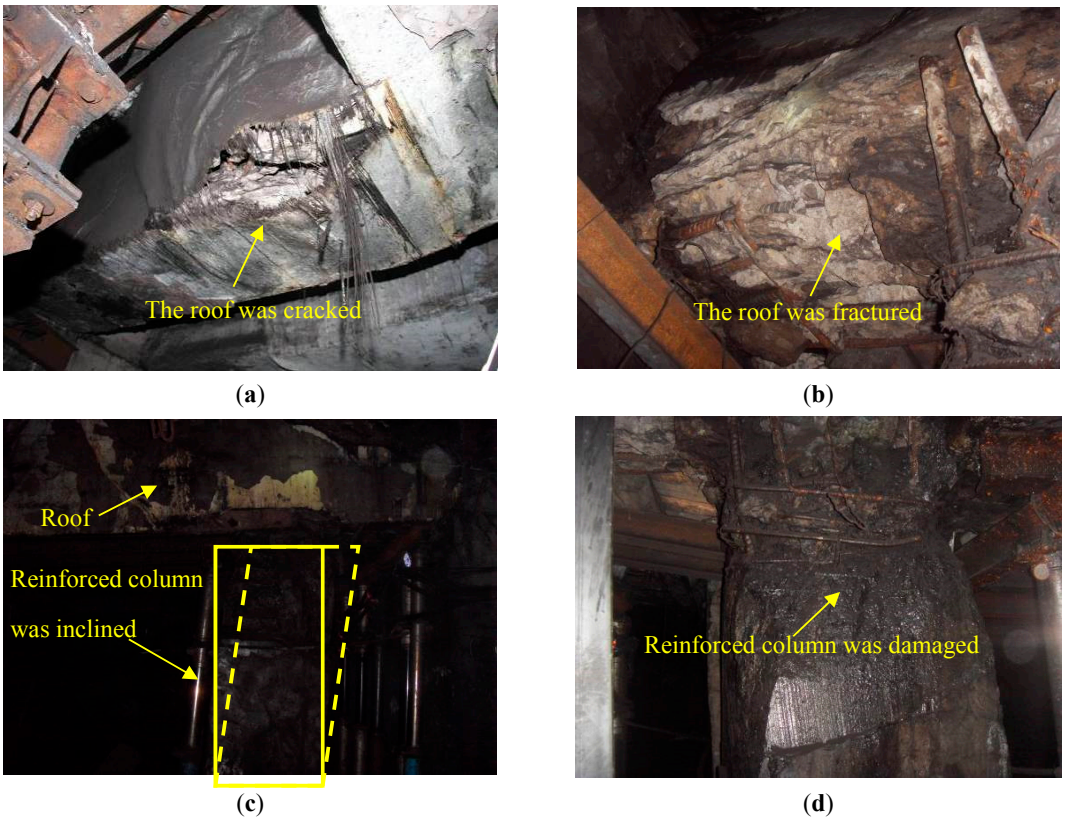

Figure 2. The collapse characteristics of the CGC: (**a**) the roof was cracked; (**b**) the roof was fractured; (**c**) the reinforced concrete column was inclined; (**d**) the reinforced concrete column was damaged.

2. Background

As shown in Figure 3, the 214# and 3# coal bunkers (the new bunker), both vertical bunkers, are located in the belt haulage roadway near the 953 sump in Xiashijie coal mine, Tongchuan Coal Mining Group Co. Ltd. The 214# coal bunker is the original coal storage bunker, with a height and diameter of 8.7 m and 5 m, respectively. It is noted that the 214# coal bunker is located entirely within 4-2# coal seam, and the two walls of CGC surrounding rock are also part of the 4-2# coal seam, and the floor is mudstone. The 3# coal bunker, also a wall-mounted coal bunker (WMCB), is built to replace the 214# coal bunker after its repeated failures. The 3# coal bunker is 5 m in diameter and 15 m in height, its upper surrounding rock is coarse sandstone and siltstone, of which the thicknesses are 3.2 m and 5.8 m, respectively. The lower part of the surrounding rock is the 4-2# coal seam, with its thickness being 6 m.

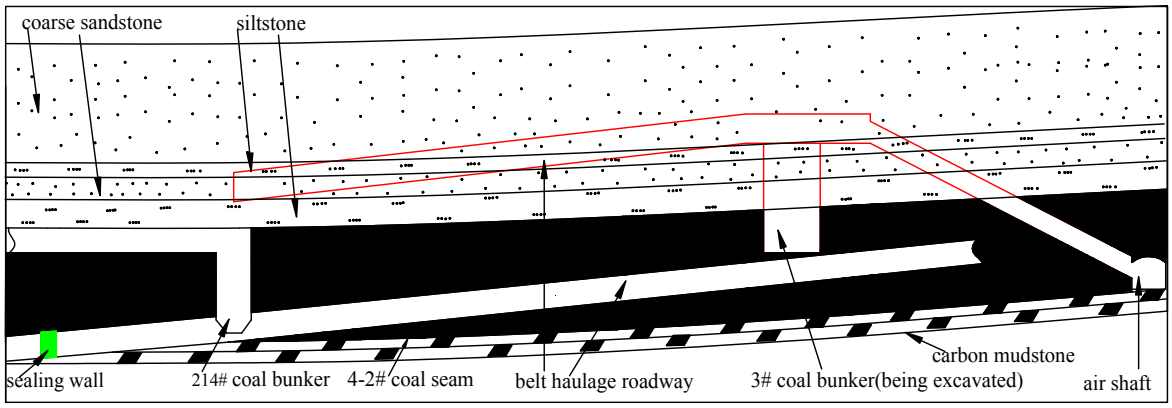

Figure 3. The geological cross-section through the 214# coal bunker and 3# coal bunker.

Preprints (www.preprints.org) | NOT PEER-REVIEWED | Posted: 20 October 2017 doi:10.20944/preprints201710.0141.v1

3. The CGC failure mechanism and its main influencing factors

3.1. Deformation characteristics of the CGC

The CGC's load-bearing structure is composed of the roof, floor and the side walls, which are made of reinforced concrete. Figure 2 shows the deformation and collapse of the CGC, even though the CGC had been repaired two times and reinforced by building a concrete column between the walls. The convergence of the chamber had been measured by crossing method (Figure 4) [19] after the latest repair. The deformation data collected after monitoring for three months is shown in Figure 5, the cumulative heave and the convergence of CGC walls are 1.632 m and 0.668 m, respectively. Based on the on-site collapse features and the deformation data, we can conclude the main deformation characteristics were as follows:

(1) Large deformation of the floor. The cumulative floor heave is much greater than the deformation of the walls in the CGC.

(2) The collapse and failure of the surrounding rock of the CGC (especially the floors) constantly emerge after repair. The load-bearing structure of the CGC could only remain stable for three months after repair (the immediate floor and hard floor are mudstone and clay, respectively, which are soft in nature and will swell severely when water is encountered).

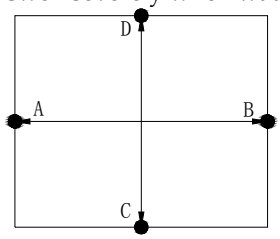

Figure 4. The crossing method of CGC displacement measurement.

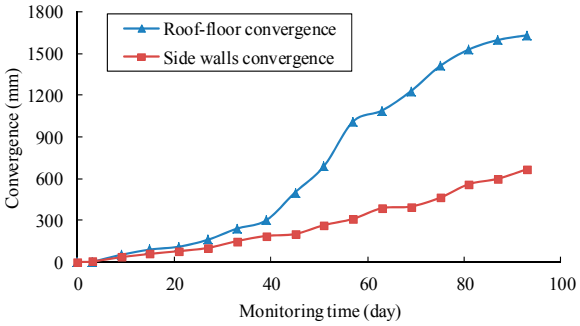

Figure 5. CGC deformation monitoring results.

3.2. Main influencing factors

According to the in situ survey and rock expansion experiments, the main factors inducing failure of the CGC are:

(1) The swelling clay of the CGC floor rock. The swelling properties of the mudstone and clay were verified by the laboratory tests such as rock expansion experiments (Figure 6 (a)), mineral composition analysis by electron microscope, and X-ray diffraction [20], and the results are shown in Table 1. Figure 6 (b) shows the rapidity of the dilatational velocity of the floor strata, and the dilatational strain increases after immersion in water for 2 h, and then it reaches the maximum of 11700 uε after 12 h. Table 1 indicates that the mudstone and clay contain abundant minerals such as kaolinite, montmorillonite, illite, etc. The clay minerals contained in the immediate floor and hard floor account for as much as 82% and 85%, respectively, which indicates that the floor rocks are liable to swell rock which is not conducive to chamber stability.

(2) The rich supply of mine water under these geological conditions. With continuous supply of water from the seepage of yellow slurry in working face goafs, the 953# sump above, and the productive water in the belt roadway (Figure 3), the swelling floor rock will have low strength

Preprints (www.preprints.org) | NOT PEER-REVIEWED | Posted: 20 October 2017 doi:10.20944/preprints201710.0141.v1

and generate a significant expansive force, thus constantly increasing the deformation: the concrete walls and floor of the chamber were crushed after repair and reinforcement, further causing the collapse in the roof of the chamber and inducing instability of the whole bearing structure of the chamber.

(3) The large ground stress due to the burial depth (400 m) and abutment pressure because of the surrounding working face goafs. The high pressure would aggravate the deformation of the surrounding rock.

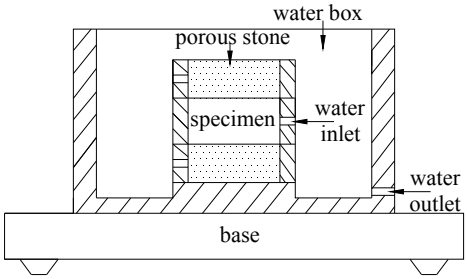

(**a**)

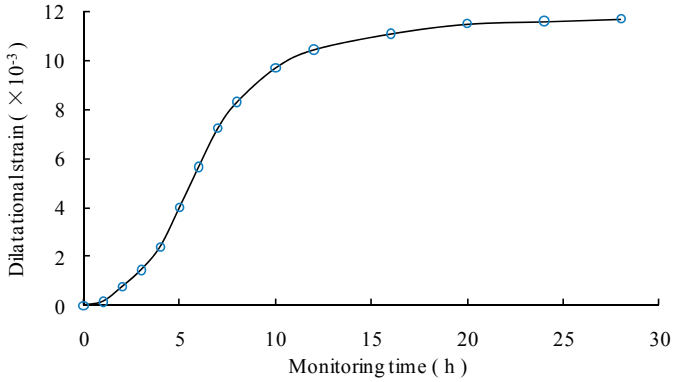

(**b**)

Figure 6. The rock expansion experiment: (**a**) Test apparatus; (**b**) Experimental results.

Table 1. Mineral composition in floor strata

Floor strata	Kaolinite (%)	Illite (%)	Montmorillonite (%)	Mixture of illite and montmorillonite (%)	Others (%)
Mudstone	23	11	6	42	18
Clay	18	12	7	48	15

3.3. The influence of floor heave on the load-bearing structure in CGC

Numerical simulation, as a basic method, is widely used to determine the stresses or displacements in underground spaces [21-22], and to analyse the failure mechanism or stability of engineering rock masses [9,23-26], to optimise support schemes for roadways [19], and to simulate experimental tests and verify the results thereof [20], etc. In this study, the influence of floor heave on the load-bearing structure in CGC was investigated by utilising FlAC^{2D} software, especially to assess the effect of water on floor heave. The coal and rock mass properties were determined by use of the Hoek-Brown failure criterion [27]: the value of GSI was obtained from the GSI chart [28]. Additionally, we selected a strain-softening model to simulate the uniaxial compression test, and the results were compared with experimental data. The simulation test results of stress-strain characteristics were changed until consistent with those of uniaxial compression tests. The coal and rock physical and mechanical parameters used in this model are shown in Table 2. During numerical modelling, the normal stiffness (k_n) and shear stiffness (k_s) of the interface between the concrete and surrounding rock could be determined by the following equation [29]:

Preprints (www.preprints.org) | NOT PEER-REVIEWED | Posted: 20 October 2017 doi:10.20944/preprints201710.0141.v1

$$k_n = k_s = 10\left[\frac{K + \frac{4}{3}G}{\Delta z_{\min}}\right] \quad (1)$$

Where K and G are the bulk and shear moduli, respectively; ΔZ_{min} is the smallest width of an adjoining zone in the normal direction (Figure 7).

To understand the influence of mine water on the failure of the CGC, the distribution of both plastic zones (Figure 8) and displacement (Figure 9) of the load-bearing structure in CGC were simulated under conditions with, and without water. As shown in Figure 8, due to mine water being encountered, the strength of the floor rock was decreased and swelling rock generated significant expansive forces, a wide ranging plastic zone appeared in the floor and walls. With the floor rock bulging out, the bottom beam was almost completely in a state of tensile failure. While the bottom beam bulged and failed, thus column was also subject to extrusion, and severe dilatancy. Finally part of the column failed in tension.

In addition, comparison of displacement distributions in load-bearing structures, with and without water (Figure 9) showed the displacement of the chamber was affected by mine water to a much greater extent than that without. Figure 9 (b) shows that, the deformation of the surrounding rock was mainly a result of roof subsidence, and overall deformations were small. As shown in Figure 9 (a), a large amount of floor heave appeared, while the deformations of the roof and two sides were small, which was in good agreement with in situ monitoring data (Figure 5). In summary, the floor heave, caused mainly by mine water, is the underlying cause of the instability and repeated failure of CGC in the 214# coal bunker.

Even though many measures such as drainage, installation of U36 steel inverted arches, reinforcement of the bottom beams and other measures had been taken, it was still difficult to control the floor heave, thus the bearing structure of the CGC could not work properly.

Table 2. The physical and mechanical parameters of surrounding rock and concrete.

Strata	Density (kg·m-3)	Bulk modulus (GPa)	Shear modulus (GPa)	Friction angle (°)	Cohesion (MPa)
Coarse sandstone (roof 3)	2600	5.0	4.0	28	2.0
Fine sandstone (roof 2)	2500	4.0	3.0	26	1.7
Siltstone (roof 1)	2550	3.5	2.5	24	1.5
4-2# coal seam	1400	1.3	0.9	18	0.3
Mudstone (floor 1)	1800	2.0	1.5	25	0.7
Clay (floor 2)	1500	2.0	1.3	23	0.3
Reinforced concrete	2700	5.0	4.0	32	2.2

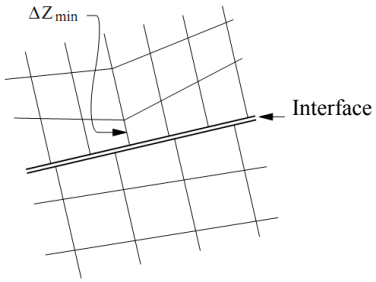

Figure 7. Zone dimensions used in stiffness calculations.

Preprints (www.preprints.org) | NOT PEER-REVIEWED | Posted: 20 October 2017 doi:10.20944/preprints201710.0141.v1

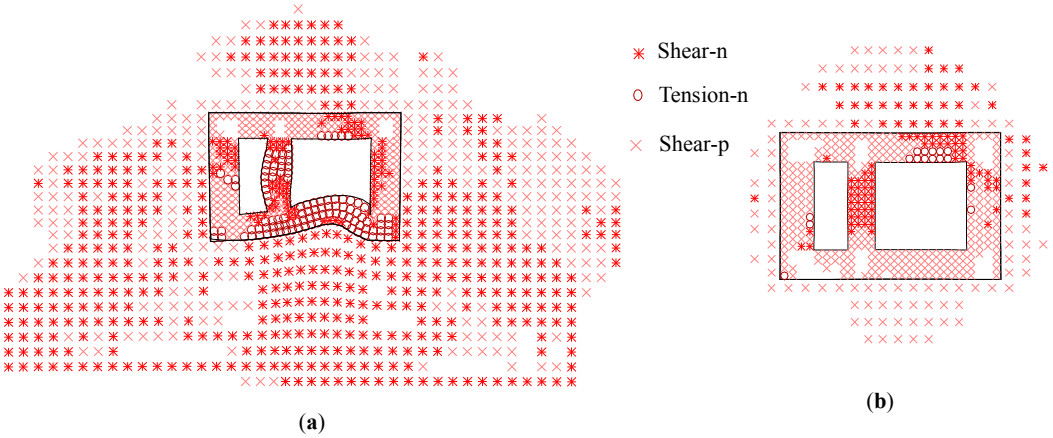

Figure 8. Comparison of plastic zone distribution in load-bearing structure (**a**) with water and (**b**) without water.

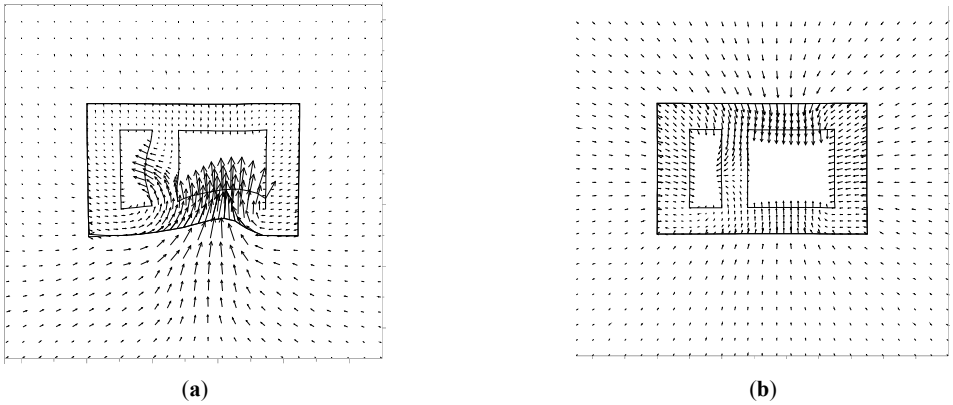

Figure 9. Comparison of displacement distribution in load-bearing structure (**a**) with water, (**b**) without water.

4. The key properties of the wall-mounted coal bunker

As discussed previously, the severe floor heave is the main factor inducing the instability of the CGC. It is necessary to design a new coal bunker without building the coal given chamber to replace the 214# coal bunker under these geological conditions. Then the invented WMCB transfers the weight borne by the load-bearing structure of the CGC to the self-bearing system established in the rock surrounding the bunker.

4.1. The reinforcement of the rock surrounding the coal bunker

The rock surrounding the bunker, in which a variety of load-bearing structures of the coal bunker will be built, should be controlled so as to develop a WMCB. So FLAC^{3D} models were established to analyse the stability of the rock surrounding the 3# coal bunker based on its geological conditions. As shown in Figure 10, the model size is 80 m × 40 m × 15 m. The simulation results (Figure 11) indicate that: (1) the surrounding rock in sandstone segments is basically stable, and the cumulative rock deformation is small. (2) The surrounding rock in coal seam segments, which moves into the inside of the bunker with a large surrounding rock deformation zone seen, is the main area of deformation in the entire surrounding rock mass: this is consistent with the results of field investigation.

To ensure the long-term stability of the surrounding rock and supporting structures, both the supporting strength and stability of the supporting structures should be taken into account. At the same time, the bolt–cable combined supporting technology [30] was adopted to control the deformation and failure of the rock surrounding the coal bunker. Significant attention should be

Preprints (www.preprints.org) | NOT PEER-REVIEWED | Posted: 20 October 2017 doi:10.20944/preprints201710.0141.v1

paid to supporting the rock surrounding the 4-2# coal seam. Specific reinforcement measures were as taken follows:

(1) A more rigid net was used to increase the rigidity of supporting sets for the coal seam segment;
(2) The thickness of the support bearing structure formed by bolting and wire mesh was increased by increasing the length of the bolt;
(3) Apart from the high prestressed anchor net supporting sets for the coal seam segment, the compensation anchors were used to reinforce the support bearing structure, which improved the stability of the supporting structure formed by bolting and wire mesh, so as to control the deformation of the rock surrounding the coal seam segment, thus ensuring the stability of the overall rock mass around the bunker.

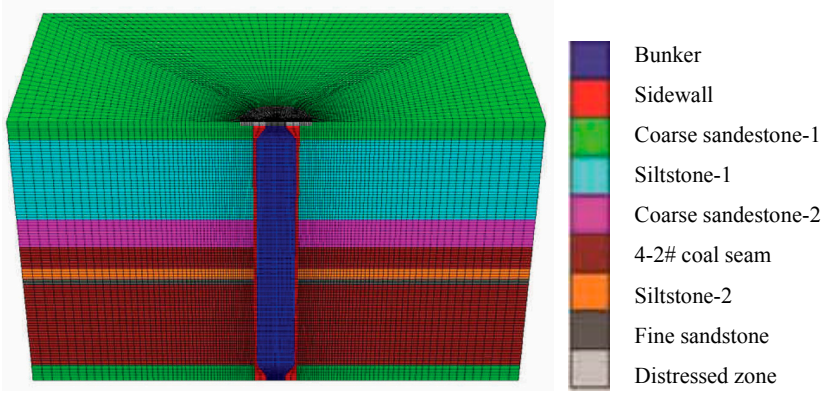

Figure 10. The FLAC^{3D} model of the 3# coal bunker.

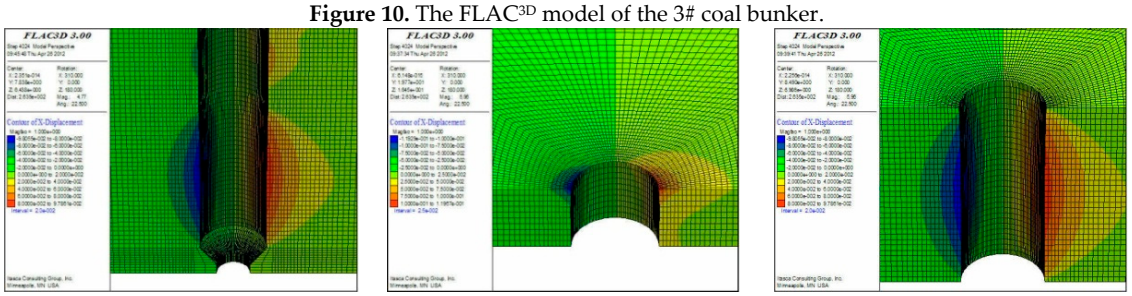

(**a**) (**b**) (**c**)

Figure 11. The surrounding rock deformation of (**a**) the whole bunker; (**b**) the sandstone segment; (**c**) the 4-2# coal seam segment in the 3#coal bunker.

Table 3. Six different reinforcement schemes.

Scheme (no.)	Bolt	Anchor cable	Cable interval
1	Φ20 × 2400mm	Φ17.8 × 5000mm	800 × 800mm
2	Φ20 × 2400mm	Φ17.8 × 5000mm	1600 × 800mm
3	Φ20 × 3000mm	Φ17.8 × 6200mm	800 × 800mm
4	Φ20 × 3000mm	Φ17.8 × 6200mm	1600 × 800mm
5	Φ20 × 3600mm	Φ17.8 × 7300mm	1600 × 800mm
6	Φ20 × 3600mm	Φ17.8 × 7300mm	1600 × 1600mm

Table 4. Plastic zone range.

Scheme (no.)	The sandstone segment (m)	The 4-2# coal seam segment (m)
1	6.1	8.9
2	6.8	9.8
3	5.2	7.6
4	5.5	7.9
5	5.3	7.5

Preprints (www.preprints.org) | NOT PEER-REVIEWED | Posted: 20 October 2017 doi:10.20944/preprints201710.0141.v1

6	5.8	8.2

Based on the measures discussed above, we designed six reinforcement schemes (Table. 3) and the numerical simulation results were shown in Table. 4. The plastic zone range of the coal seam segment decreases significantly from 9.8 m to 7.6 m when the length of the bolt increases from 2.4 m to 3.0 m and that of cable increases from 5.0 m to 6.2 m, respectively, however, the plastic zone extent then decreases to an insignificant extent when using longer bolts and cables. Comparison of Schemes 5 and 6 shows that the reinforcing interval of the grouted anchor cables have a significant effect on the size of the plastic zone. So the reinforcing interval was selected as 1600 × 800 mm. Finally, an optimised scheme was realised (Figure 12) considering the cost, installation convenience, and technical feasibility. Figure 12 shows that:

(1) The bolt and wire mesh were used to reinforce the shallow rock and coal at intervals of 800 mm × 800 mm, and the bolt tightening torque was not less than 300 N•m.
(2) The bearing capacity of deep surrounding rock was aroused by the anchor cable (Φ17.8mm × 6200 mm) with the spacing and row spacing being 1600 mm × 800 mm.
(3) At the same time, Φ14 mm ladder beams, along the periphery of the wellbore, were used to link the bolts and anchors, thus the overall stability of the supporting system was enhanced. The H-steel brackets, which were used to form the coal bunker funnel (Figure 12) and improve the supporting effect on the surface of the surrounding rock, were fastened to the wall by the Φ21.8 mm × 6200 mm anchor cables.
(4) Additionally, the Φ21.8 mm × 10,000 mm self-locking anchor cables (Figures 12, 13, 14 and 15), also used as compensation anchors, were reinforced to improve the stability of the supporting structure formed by bolting and wire mesh in the coal seam segment to serve as the auxiliary carrying system able to bear the full weight of the coal bunker with the main bearing system, which ensured the long-term stability of the coal bunker.

4.2. The self-bearing system of the coal bunker

4.2.1. The main bearing system

The H-steel beams, installed in the sandstone rock uniformly, bear the whole weight of the 3# coal bunker without considering friction and adhesion between the concrete (Figures 1(b) and 13) and the surrounding rock, so it is necessary to ensure that the carrying capacity of H-steel beams (Figure 14) was greater than the total weight of the coal bunker with a certain safety factor. This computation may be summarised as follows:

The bunker total weight is:

$$M_T = M_{C1} + M_{C2} + M_B + M_F \tag{2}$$

where M_{C1}, M_{C2}, M_B and M_F are the weight of coal when the coal bunker is filled, the weight of concrete, the total weight of the H-steel brackets, the weight of the feeder, respectively, and the weight borne by each H-steel beam is:

$$M = \frac{M_T}{n} \tag{3}$$

where n is the number of H-steel beams buried in the bunker wall rock. Then the shear stress on the section of the H-steel beam is:

$$\tau = \frac{Mg}{S} \tag{4}$$

where S is the cross-sectional area of the H-steel beam.

Thus, the safety factor can be given by:

Preprints (www.preprints.org) | NOT PEER-REVIEWED | Posted: 20 October 2017 doi:10.20944/preprints201710.0141.v1

$$n_s = \frac{[\tau]}{\tau} \tag{5}$$

where [τ] is the allowable shear stress in the H-steel beam.

As discussed above the lower part of the surrounding rock is the 4-2# coal seam with its low strength: to facilitate the formation of the funnel and enhance the overall stability of the structure of the bunker, the H-steel brackets are installed uniformly in the rock along the periphery of the wellbore (Figure 13). The upper ends of the H-steel brackets are embedded into the stable surrounding rock in the upper portion of the coal bunker; the bottom parts of brackets are fitted together to form the skeleton of the coal hopper. Additionally, the upper portions of H-steel brackets are fixed to the rock by the anchor cable, thus not only transferring the bearing capacity of the deep rock and improving the stability of the shallow surrounding rock, but also enhancing the stability of the frame formed by these H-steel brackets.

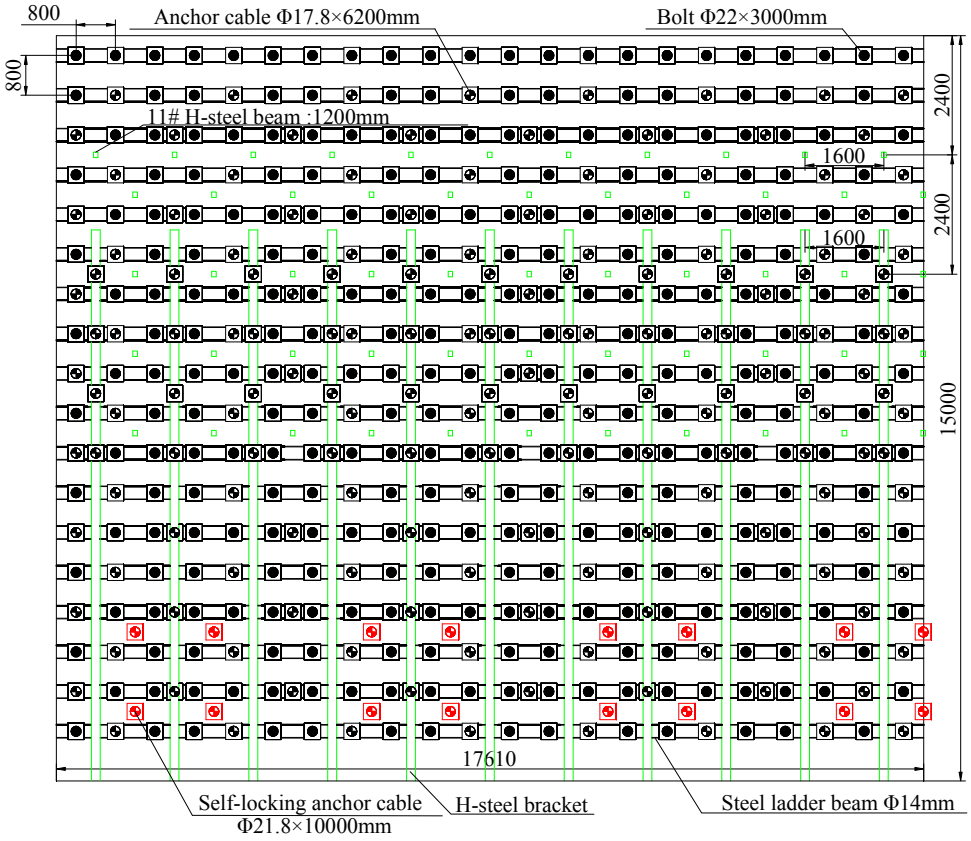

Figure 12. The supporting scheme for the coal bunker.

Preprints (www.preprints.org) | NOT PEER-REVIEWED | Posted: 20 October 2017 doi:10.20944/preprints201710.0141.v1

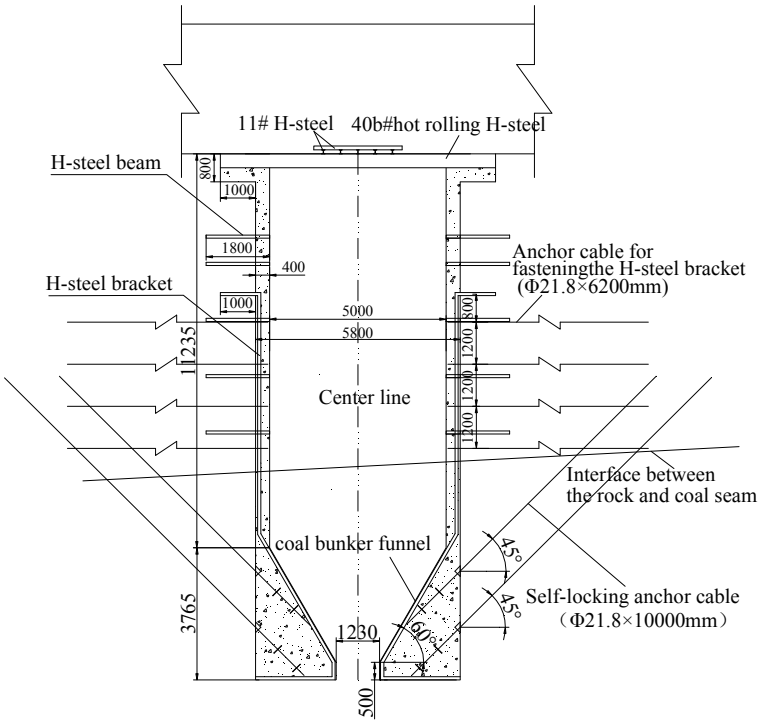

Figure 13. Schematic diagram of the WMCB.

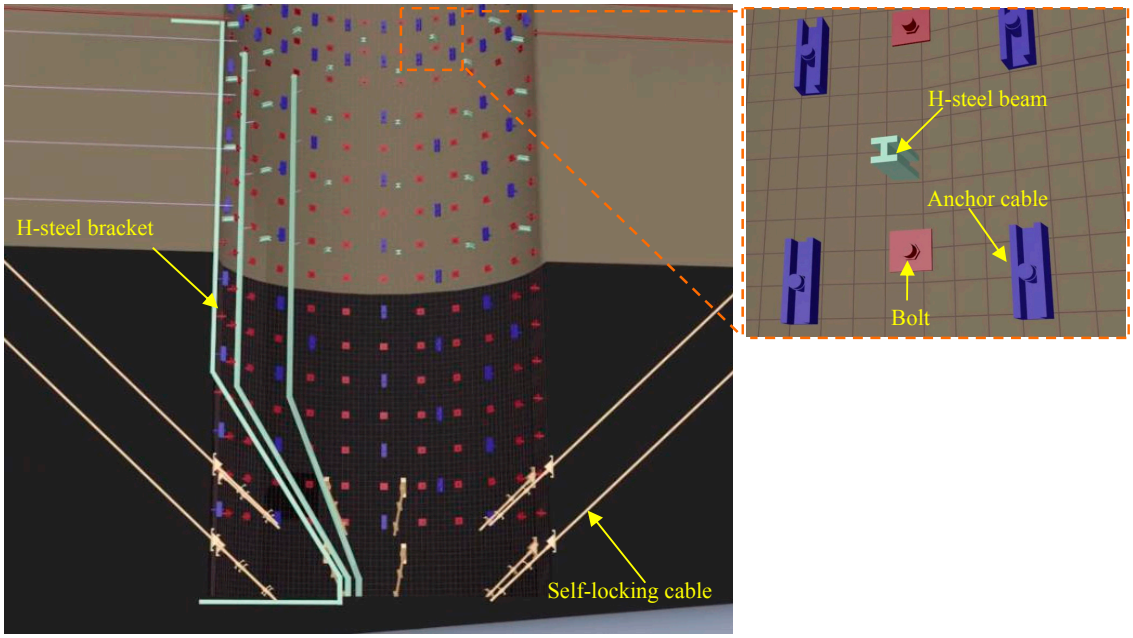

Figure 14. A 3-d view of the structure of the WMCB.

4.2.2. The assisted bearing system

The assisted bearing system, which includes 16 self-locking anchor cables (Figure 15) arranged uniformly in the bunker funnel portion along the bunker wall rock, is also designed to enhance the stability of the bunker. Thus the weight of the bunker funnel is borne by the deep stable surrounding rock with the self-locking anchor cable anchored therein, ensuring the long-term stability of the coal bunker. Figure 15 shows the sample structure of the self-locking anchor cable. Since the vertical component force of the self-locking anchor cable is provided as follows,

Preprints (www.preprints.org) | NOT PEER-REVIEWED | Posted: 20 October 2017 doi:10.20944/preprints201710.0141.v1

$$F_v = nF\sin\alpha \tag{6}$$

where n is the number of self-locking anchor cables, F_v is the vertical component force provided by the self-locking anchor cable, F is the single anchor bearing capacity, and α is the angle between the cable and the rock face, then suppose that the whole weight of the bunker is borne by the self-locking anchor cables, the safety factor can be given by:

$$K = \frac{F_v}{M_T \mathrm{g}} \tag{7}$$

The safety factor $K > 1$, thereby determining the number of self-locking anchor cables.

With the surrounding rock deformation effectively controlled, the reinforcement is implemented depending on the intensity of bunker body, then the H-steel beams, H-steel brackets, and the self-locking anchor cables are immersed in the concrete to form a WMCB (Figure 15, 1(b)).

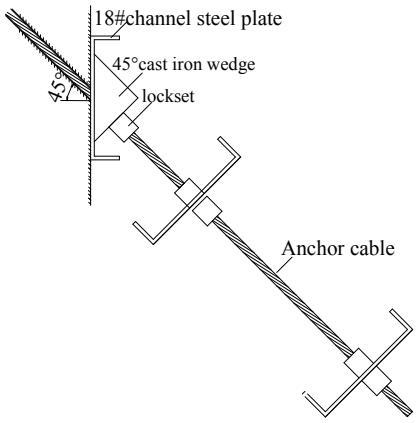

Figure 15. A typical self-locking anchor cable.

4.2.3. Safety assessment

The bunker body height and high hopper are 11235 mm and 3765 mm, respectively: the total thickness of concrete is not less than 400 mm, and the concrete strength is 40 MPa.

The total weight (concrete, coal, and coal feeder beam) is calculated as follows:

Coal funnel volume: $V_1 = \frac{1}{3}\pi H_1\left[\left(\frac{D_1+b_1}{2}\right)^2 - \frac{D_1 b_1}{4}\right]$; Bunker volume: ;Concrete volume: $V_2 = \frac{1}{4}\pi D^2 H - Q$;

Concrete volume: $V_2 = \frac{1}{4}\pi D^2 H - Q$; Coal weight: $M_{C1} = \rho_{c1} V_2 Q$; Concrete weight: $M_{C2} = \rho_{c2} V_2$; The total weight of the H-steel brackets: $M_B = P_l n_B L_B$;

Where H is the bunker design height, 15 m; H_1 is the coal funnel height, 3.765 m; H_2 is the bunker body height, 11.235 m; D is the section diameter of the bunker, 5.8 m; D_1 is the net cross-sectional diameter of the bunker, 5 m; b_1 is the mouth width of the funnel, 1.23 m; the weight of coal feeder is 4.5 t; P_l is the lineal density of the H-steel, 26.05 kg/m; L_B is the H-steel bracket length, 15.013 m, n_B is the number of H-steel barn brackets, 12; and ρ_{c1} and ρ_{c2} are the density of the coal (1.4 t/m^3) and concrete (2.7 t/m^3), respectively.

These data are substituted into Eq. (2), then M_T can be calculated as follows: M_T = 777.1 t. With the number (60) of H-steel beams and cross-sectional area (0.003318 m^2), and an allowable shear stress of 125 MPa, substituting these into Eqns (3), (4) and (5), safety factor: $n_s = \frac{125}{38.25} = 3.26 > 2$, thus meeting safety requirements.

Preprints (www.preprints.org) | NOT PEER-REVIEWED | Posted: 20 October 2017 doi:10.20944/preprints201710.0141.v1

The diameter of the self-locking anchor cable is 21.8 mm, with its carrying capacity being 458 kN. Substituting these data into Eqns (6) and (7), safety factor: $K=\frac{10361.792}{777.1\times9.8}=1.36>1'$ meeting safety requirements.

5. WMCB application

Currently, the wall-mounted bunker has been in operation for three years. Long-term monitoring data (Figure 16) and site observation show that: the cumulative subsidence of the bunker body is 64 mm, and the coal bunker diameter convergence measured by crossing method is 51.5 mm; no cracking was seen after application of the WMCB.

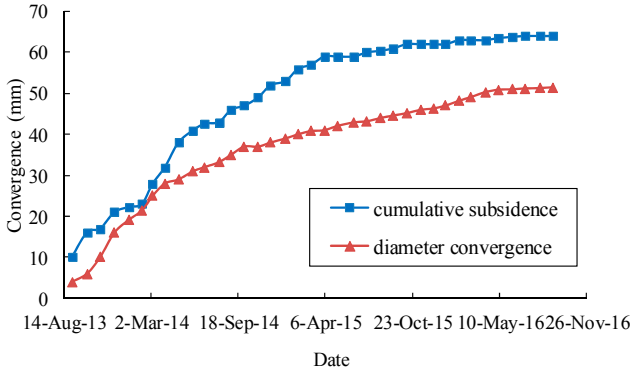

Figure 16. Bunker settlement and convergence of the diameter monitoring.

6. Discussion

In this study, the factors, which cause the floor heave and the collapse of the load-bearing structure in the CGC, are investigated by FLAC2D numerical modelling and expansion experiments. Then the WMCB is designed to avoid the influence of the floor heave and a self-bearing system, which includes H-steel beams, H-steel brackets, and self-locking anchor cables, forms a replacement for the CGC to bear the whole weight of the bunker, so that the whole weight is transferred to the stable surrounding rock. The stability of the new coal bunker has been verified in Xiashijie coal mine, and it has made coal production therein more efficient.

The great economic benefits, due to the application of the WMCB, are shown in Table 5. As the 214# coal bunker should be repaired for a month every year, and the annual production capacity of the mine is 2.4 million tons, the use of the WMCB gives rise to a production increase of more than two hundred thousand tons of coal every year (an economic benefit of 52 million RMB at a unit-price of 260 RMB per ton). Besides, the application of the WMCB reducing costs for construction and maintenance of the original CGC, even though the construction cost of the WMCB is 3.909326 million RMB, the coal mine has gained economic benefit amounting to 158.026174 million RMB over three years.

Comparison of the WMCB and the traditional vertical coal bunker shows the differences between them in that the former is a new vertical coal bunker without the CGC and can remain stable when the floor heave is severe or the strength of the floor rock is especially low, thus the new coal bunker is a better solution to the floor heave issue. Until now, no vertical coal bunker without a CGC has been reported. The new coal bunker, stable and easy to maintain, offers great potential for application in mines with similar geological conditions.

Table 5. Calculation of the economic benefits.

The cost of repair and maintenance of 214# coal bunker (million RMB)	Economic benefits from production increase every year (million RMB)	The construction cost of the WMCB (million RMB)	Net economic benefit over three years (million RMB)
1.9785	52	3.909326	158.026174

7. Conclusions

(1) The results of expansion testing and numerical simulation analysis indicated that the floor heave, caused mainly by mine water, was the basic reason for the instability and repeated failure of the coal given chamber in the 214# coal bunker.

(2) The WMCB was designed to replace the 214# coal bunker and the stability of its surrounding rock was simulated and analysed. The results showed that the surrounding rock in the coal seam segment formed the main deformation area in the entire rock mass surrounding the bunker. Then the surrounding rock was controlled by means of a high-strength bolt–cable combined support system. The self-bearing system of the wall-mounted bunker is composed of H-steel beams, H-steel brackets with fixed anchors, and self-locking anchor cables able to bear the whole weight of coal bunker by utilisation of stable surrounding rock, thus negating the need for a bearing structure at the bottom of coal given chamber.

(3) The WMCB differs from the traditional coal bunker in that the former, without the CGC, is easier to maintain than the latter when the floor rocks is soft and prone to swelling.

(4) Field testing proves that the WMCB, being stable and safe, contributed to a significant enhancement of production without repair to the CGC for one month in every year. The coal mine has accrued economic benefits amounting to 158.026174 million RMB over three years.

(5) It is primary to establish the WMCB rather than the traditional coal bunker under geological conditions encompassing such severe floor heave, loose (or fractured) floor rock, and the other similar conditions. The WMCB offers great prospects for application in other mines subject to similar geological conditions.

Acknowledgments: The work presented in this paper is financially supported by State Key Laboratory of Coal Resources and Safe Mining, China University of Mining and Technology (No. SKLCRSM15X01). We wish to thank the Xiashijie Coal Mine for supporting to conduct this important study, as well as Xiaoquan Huo, Ming Xu for the assistance of field construction and data collection.

Author Contributions: All the authors contributed to publishing this paper. Xingkai Wang performed the numerical analysis and prepared the manuscript. Wenbing Xie proposed the new coal bunker and its key reinforcement techniques. Jianbiao Bai and Shengguo Jing revised the manuscript. Zhili Su participated the data processing during the research process.

Conflicts of Interest: The authors declare no conflict of interest.

References

1. Alotin, L.M.; Belgorodskii, V.L. Practice and theory of improving coal output by the use of a storage bunker in the transporation line. *Soviet Min. Sci.*, **1971**, 6, 700-702, DOI: 10.1007/BF02507571.
2. Liu, F. Research on failure mechanism and its control technology of shaft coal pocket. A master's thesis. Chongqing University, Chongqing, 2008. (in Chinese with English abstract)
3. Sureshc, B.; Carlos, D.; Michael, H. Optimum bunker size and location in underground coal mine conveyor systems. *Int. J. Min. Geo. Eng.*, **1987**, 5, 391-404, DOI: 10.1007/BF01552753.
4. Wang L. Analysis and caculation of capacity of underground coal bunker. *Jounal of Huainan Mining*, **1983**, 1, 113-122. (in Chinese)
5. Shramko, V.M. Influence of the collection bunker capacity to the utilization level of the main mine subsystems. *Soviet Min. Sci.*, **1984**, 20, 489-492, DOI: 10.1007/BF02498206.
6. Duckmanton, F.; Carlin, R. Vertical bunker. *Colliery Guardian Redhill*, **1986**, 234, 444-446.
7. Cui, Q.A.; Shen, J.J. Location selection of coal bunker based on particle swarm optimization. The Paper Presented on The 19th International Conference on Industrial Engineering. Berlin, Heidelberg, Germany, 2013. Chapter 119; pp. 1121-1128.
8. Ma, W.F.; Chen, J.S.; Zhao J.C. Large-scale coal bunker engineering practice in deep shaft. Shanxi Archit, **2012**, 38, 117-118. (in Chinese)
9. Ma, H.T. Design and construction technology of coal bunker with large diameter and high vertical height. Coal Eng., **2015**, 47, 42-44. (in Chinese with English abstract)
10. Li, Z.Q. FEM application to loess slope excavation and support: case study of Dong Loutian coal bunker, Shuozhou, China. *Bull. Eng. Geol. Environ.*, **2014**, 73, 1013-1023, DOI: 10.1007/s10064-013-0564-6.

11. Wang, H. Study on water inrush prevention technology of temporary coal bunker construction. *Coal Eng.*, **2013**, 16, 46-48. (in Chinese with English abstract)
12. Lv, H.L.; Ma, Y.; Zhou S.C.; Liu, K. Case study on the deterioration and collapse mechanism and curing technique of RC coal bunkers. Procedia *Earth and Planetary Sci.*, **2009**, 1, 606-611, DOI: 10.1016/j.proeps. 2009.09.096.
13. Dong, R.Q. Anti failure technology of 100 m high vertical coal silo. *Coal Sci. Technol.*, **2009**, 37, 18-21. (in Chinese with English abstract)
14. Gong Q. A study on coal bunker dredging technology under highly dynamic pressure and a portable dredger. *China Coal*, **2008**, 34, 67-69. (in Chinese with English abstract)
15. Gong Q. Analysis on blockage of coal bunker and its prevention. *Min. Processing Equipment*, **2008**, 36, 24-26. (in Chinese with English abstract)
16. Sun, J.P.; Jiang, J. Laser monitoring of the coal level of coal silo by depth pre-calibration. *J. China Coal Soc.*, **2012**, 37, 172-176. (in Chinese with English abstract)
17. Song, Z.A.; Zhan, F.; Li, C.Y. Research of the underground coal bunker clearing robot. *J. Coal Sci. Eng.*, **2010**, 16, 104-107, DOI: 10.1007/s12404-010-0120-y.
18. Zhao, X.L.; Shen, J.W.; Shang W.W. Practice and research on natural ventilation of cylindrical coal bunker for gas exhaust. *Coal Eng.*, **2014**, 46, 137-139. (in Chinese with English abstract)
19. Wang, F.T.; Zhang, C.; Wei, S.F.; Zhang, X.G.; Guo, S.H. Whole section anchor-grouting reinforcement technology and its application in underground roadways with loose and fractured surrounding rock. *Tunn. Undergr. Space. Technol.*, **2016**, 51, 133-143, DOI: 10.1016/j.tust.2015.10.029.
20. Yang, S.Q.; Chen M.; Jing H.W.; Chen K.F; Meng B. A case study on large deformation failure mechanism of deep soft rock roadway in Xin'An coal mine, *China. Eng. Geol.*, **2017**, 217, 89-101, DOI: 10.1016/j.enggeo.2016.12.012.
21. González-Nicieza, C.; Menéndez-Díaz, A.; Álvarez-Vigil, A.E.; Álvarez-Fernández, M.I. Analysis of support by hydraulic props in a longwall working. *Int. J. Coal. Geol.*, **2008**, 74, 67–92, DOI: 10.1016/j.coal.2007.10.001.
22. Liang, S.; Elsworth, D.; Li, X.H.; Fu, X.H.; Sun, B.Y.; Yao, Q.L. Key strata characteristics controlling the integrity of deep wells in longwall mining areas. *Int. J. Coal. Geol.*, **2017**, 172, 31– 42, DOI: 10.1016/j.coal.2017.01.012.
23. Álvarez-Fernández, M.I.; González-Nicieza, C.; Álvarez-Vigil, A.E.; García, G. H.; Torno, S. Numerical modelling and analysis of the influence of local variation in the thickness of a coal seam on surrounding stresses: Application to a practical case. *Int. J. Coal. Geol.*, **2009**, 79, 157– 166, DOI: 10.1016/j.coal.2009.06.008.
24. Campbell, R.; Mouldb, R.J. Impacts of gloving and un-mixed resin in fully encapsulated roof bolts on geotechnical design assumptions and strata control in coal mines. *Int. J. Coal. Geol.*, **2005**, 64, 116–125, DOI: 10.1016/j.coal.2005.03.009.
25. Gentzis, T.; Deisman, N.; Chalaturnyk, R.J. A method to predict geomechanical properties and model well stability in horizontal boreholes. *Int. J. Coal. Geol.*, **2009**, 78, 149-160, DOI: 10.1016/j.coal.2008.11.001.
26. Ma, D.; Miao, X.X.; Bai, H.B. Effect of mining on shear sidewall groundwater inrush hazard caused by seepage instability of the penetrated karst collapse pillar. *Nat. Hazards*, **2016**, 82, 73-93, DOI: 10.1007/s11069-016-2180-9.
27. Hoek, E.; Brown, E.T. Practical estimates of rock mass strength. *Int. J. Rock Mech. Min. Sci.*, **1997**. 34, 1165-1186, DOI: 10.1016/S0148-9062(97)00305-7.
28. Marinos, P.; Hoek, E. GSI: a geologically friendly tool for rock mass sthrength estimation. Proceeding for the Geo. Eng. 2000 at the International Conference on Geotechnical and Geological Engineering. Technomic Publishers, Lancaster, Melbourne; pp. 1422-1446.
29. Itasca consulting group, inc., 2005. Manual of FLAC Version 5. Itasca Consulting Group,inc., USA, Minneapolis, MN.
30. Meng, Q.B.; Han, L.J.; Sun J.W. Experimental study on the bolt–cable combined supporting technology for the extraction roadways in weakly cemented strata. *Int. J. Min. Sci. Technol.*, **2015**. 25, 113–119, DOI: 10.1016/j.ijmst.2014.11.010.